Severe convection and lightning in subtropical South America

By Kristen L. Rasmussen[1], Manuel D. Zuluaga, and Robert A. Houze, Jr.

Department of Atmospheric Sciences

University of Washington

Seattle, WA

Submitted to *Geophysical Research Letters*

September 2014

Revised October 2014

[1] *Corresponding author:* Kristen Lani Rasmussen, Department of Atmospheric Sciences, University of Washington, Box 351640, Seattle, WA 98195
E-mail address: kristen@atmos.uw.edu

KEY POINTS

- Overview of severe weather impacts from extreme storms seen by the TRMM satellite.
- Study of the seasonal, diurnal, and extreme storm-related lightning in South America.
- Preference for hail in the Andes foothills and tornadoes in the plains of central Argentina.

ABSTRACT

Satellite radar and radiometer data show that subtropical South America has the world's deepest convective storms, robust mesoscale convective systems, and very frequent large hail. We determine severe weather characteristics for the most intense precipitation features seen by satellite in this region. In summer, hail and lightning concentrate over the foothills of western Argentina. Lightning has a nocturnal maximum associated with storms having deep and mesoscale convective echoes. In spring, lightning is maximum to the east in association with storms having mesoscale structure. A tornado alley is over the Pampas, in central Argentina, distant from the maximum hail occurrence, in association with extreme storms. In summer, flash floods occur over the Andes foothills associated with storms having deep convective cores. In spring, slow-rise floods occur over the plains with storms of mesoscale dimension. This characterization of high-impact weather in South America provides crucial information for socioeconomic implications and public safety.

1. Introduction

Subtropical South America has the deepest convective storms [*Zipser et al.,* 2006] and highest frequency of large hail in the world [*Cecil and Blankenship,* 2012]. It is also the location of intense mesoscale convective systems (MCSs) [*Romatschke and Houze,* 2010; *Rasmussen and Houze,* 2011]. However, the climatology of severe weather manifested by these storms as hail, tornadoes, and floods have been relatively understudied. This short paper therefore documents the severe weather associated with extreme convective storms in subtropical South America (hereafter SSA) by correlating satellite radar and lightning data with local observations and eyewitness reports of floods, hail, and tornadoes.

TRMM Precipitation Radar (PR) data analysis has revolutionized a number of characteristics of precipitating systems in remote regions of the world that were previously unknown. SSA is one such region; the lack of a ground-based radar network until recently has limited both the study and understanding of the severe weather that occurs there. TRMM PR observations have led to the realization that intense storms just east of the Andes in SSA are among the most intense anywhere in the world [*Zipser et al*., 2006] and have shown the different forms of convection that affect the region [*Romatschke and Houze*, 2010*; Rasmussen and Houze*, 2011]. These findings raise questions regarding the climatology of severe weather events and socioeconomic impacts associated with these storms. Particularly needed are climatologies of lightning, floods, hail, and tornadoes, the primary elements of weather affecting human activity. This study presents a comprehensive overview of severe weather impacts from the most extreme storms seen by the TRMM satellite in SSA. We examine seasonal and diurnal

lightning patterns and compile the spatial distribution of flooding, hail, and tornadoes in SSA. This research provides a basis for future research into the structure and characteristics of the high-impact storms that occur in SSA.

2. Data and methodology

The TRMM PR has relatively fine three-dimensional spatial resolution (4-5 km horizontal, 250 m vertical resolution at nadir), and its areal coverage is comprehensive between 36°N and 36°S [*Kummerow et al.,* 1998]. In this study, we use sixteen years (1998-2013) of TRMM PR V7 2A25 data (radar reflectivity and rain type; *Iguchi et al.*, 2000; *Awaka et al.*, 1997) over South America in the austral spring through fall seasons. *Houze et al.* [2007] developed a technique that has been used in multiple studies in SSA [*Romatschke and Houze,* 2010; *Rasmussen and Houze,* 2011; *Rasmussen et al.*, 2013]. This method identifies three types of three-dimensional echo objects to facilitate investigation of storms containing extreme structural characteristics: 1) A deep convective core (DCC) is a contiguous volume of convective echo exceeding 40 dBZ and ≥ 10 km in height; it indicates the most locally deep and vigorous convection; 2) a wide convective core (WCC) is a contiguous 40 dBZ echo volume ≥ 1000 km^2 that indicates the presence of strong convection located within a horizontally sizable area; it suggests strong convective systems organizing onto the mesoscale, as several strong updraft cells are likely located in horizontal proximity to produce a contiguous region of heavy precipitation; and 3) a broad stratiform region (BSR) is a contiguous area of stratiform echo ≥ 50,000 km^2; it is typically associated with mature MCSs. Radar echoes that satisfy the criteria for both the DCC and WCC categories are termed deep and wide convective cores (DWCCs). In SSA, the convective categories tend to produce hail, lightning, heavy

rain, and tornadoes and the stratiform category is associated with widespread rain and flooding [*Rasmussen and Houze,* 2011]. The probability of finding these storm types during the austral summer in South America is analyzed in *Romatschke and Houze* [2010] and is updated to include probabilities during the spring through fall seasons provided by K. L. Rasmussen (manuscript in preparation, 2014).

A monthly climatology of lightning rates was calculated from the merged Lightning Imaging Sensor (LIS) and Optical Transient Detector (OTD) dataset [*Cecil et al.,* 2014] from September to May in 1998-2010. In addition, using the LIS orbital data, individual lightning flashes (fl) and the sensor viewing time (observation duration) were identified within the horizontal area projected by each TRMM-identified radar echo defined above and accumulated in a 0.05° × 0.05° grid to estimate the lightning rates from extreme storms. In addition, the raw flash count was scaled by the appropriate detection efficiency, which varies with the time of day (similar to the methodology used in *Cecil et al.,* [2014]). Finally, the lightning rate (flashes min^{-1}) was computed as the ratio between the accumulated scaled flash count and viewing time. The maps were then resampled to a coarse grid of 1° × 1° resolution to facilitate a better presentation of the high-resolution data, as has been done in other studies using LIS data [*Cecil et al.*, 2014].

To assess the occurrence of severe storms in SSA, newspaper reports in Argentina and Uruguay are used to compile data in three categories: floods, hail, and tornadoes. The newspapers that provided archived information are as follows: Clarín (www.clarin.com), Diario Los Andes (www.losandes.com.ar), La Nación (www.lanacion.com.ar), and Últimas Noticias (www.ultimasnoticias.com.uy). In each of the three storm type categories defined above, the top 100 events were selected based on the following

criteria: (1) DCC echo top height, (2) WCC echo size, and (3) BSR echo size. Queries in the above newspaper databases for the top 100 cases of each storm type extending ±1 day of the TRMM overpass time were performed and any articles related to flooding, hail, or tornadoes were identified. Then, each relevant article was examined for specific locations (e.g. town and road descriptions, distances from various cities, landmarks, etc.) to locate each storm report on a map. The resulting spatial distributions of floods, hail, and tornadoes will be presented in Section 4.

3. Lightning associated with extreme storms in subtropical South America

Assessing the severity of convective storms based on lightning frequency is a topic of great study around the world since lightning is a commonly used proxy for intense and developing storms [*Macgorman and Burgess,* 1994; *Lang and Rutledge,* 2002; *Carey et al.,* 2003]. Lightning data from the LIS aboard the TRMM satellite provides a uniform view of the lightning distribution and frequency in the subtropics and tropics. Very few studies have specifically looked at the lightning distribution in SSA, and up to now there has been a distinct lack of analysis of both seasonal and diurnal occurrence of lightning in a region that experiences some of the deepest convection on Earth. This study uses sixteen years of TRMM and LIS data over SSA to assess the seasonal, diurnal, and extreme storm-related lightning patterns.

Figure 1 presents a monthly climatology of lightning flash rates in SSA. Lightning activity in the early- to mid-spring season occurs in northeastern Argentina and southwestern Brazil (Fig. 1a-c), but in the transition to the summer season (Fig. 1d-f), lightning activity moves to the southwest into central Argentina near the Sierras de Córdoba range (between ~30 to 35°S; black outline in Fig. 1) and the Andean foothills.

Analysis of the spatial distribution of extreme storms with the TRMM PR [*Zipser et al.,* 2006*; Romatschke and Houze,* 2010] has shown that some of the deepest convection in the world occurs in the Andes foothills during the austral summer. This deep convection corresponds in location to the climatological maximum of lightning in Figure 1d-f. The lightning distribution in Figure 1c-g highlights the role of the Andes foothills in focusing convective initiation, with the Sierras de Córdoba mountains being of particular importance, as was hypothesized in *Romatschke and Houze* [2010] and *Rasmussen and Houze* [2011].

To investigate the specific relationship between lightning and specific forms of convection in South America, the seasonal patterns of lightning associated with the extreme convective forms defined above are presented in Figure 2. Strong similarities between Figures 1a-c and 2a and d indicate that storms containing both deep and wide convective cores are likely responsible for the maxima of lightning in northeastern Argentina and southwestern Brazil during the spring season. Additionally, a comparison of Figures 1c-f to Figures 2b and e indicates that the summer lightning distribution near the foothills of the Andes is associated strongly with both storms containing DCCs and storms containing WCCs. Lightning associated with BSRs is negligible (not shown).

Figure 3 shows the diurnal variation of the lightning as a function of distance from the Andes and storm type during austral summer. The maximum occurrence of lightning in storms containing only DCCs (Figure 3a), DWCCs (Figure 3b), and only WCCs (Figure 3c) are all located in the foothills of the Andes around midnight. *Romatschke and Houze* [2010] and *Rasmussen and Houze* [2011] concluded that deep convection tends to be triggered over the Andes foothills and the Sierras de Córdoba range in western

Argentina. They also concluded that the convection forming in that area starts with storms containing DCCs that move eastward over the plains, as they grow upscale into MCSs containing WCCs and broad stratiform regions. The lightning data in Figure 3 show that the lightning occurrence in storms containing DWCCs and WCCs, respectively, is found farther eastward as the systems become more mesoscale in character. Yet, all three categories of storm type retain a maximum of lightning around midnight over the foothills (cf. Figures 3a-c over the indicated topography). This indicates that as the systems expand eastward, their deep convective elements related to lightning production continue forming over the terrain as the South American Low-level Jet (SALLJ) continuously brings warm and moist air south from the Amazon into the region, impinging on the foothills and providing a lifting mechanism to break the capping inversion [*Rasmussen and Houze,* 2011]. In other words, the continuous formation of new lightning-producing cells over the foothills gives the eastward moving MCSs a back-building aspect. Terrain-locked back-building MCSs have also been observed in southwest Taiwan [*Xu et al.* 2012]; however, in that case the new cells were forming at a distance from the mountain, on the border of a cold pool continually fed by convective cells moving over the mountain. This behavior of the lightning is consistent with studies of the orogenic nature of the extreme convective systems forming in this region that has been described statistically by *Romatschke and Houze* [2010], in case studies by *Rasmussen and Houze* [2011], and will be examined via modeling in a forthcoming paper by K. L. Rasmussen (manuscript in preparation, 2014).

4. Floods, hail, and tornadoes in subtropical South America

A systematic reporting of severe weather in the region studied here has been lacking until now. However, by compiling newspaper reports of tornadoes, *Altinger de Schwarzkopf and Russo* [1982] showed that tornadoes occur in central Argentina. *Nascimento and Doswell* [2005] highlighted the need for improved documentation of thunderstorms and tornadoes in South America. In the absence of such improvement, we have drawn inspiration from *Altinger de Schwarzkopf and Russo* [1982] and have compiled storm reports for this study from the 100 most extreme storms observed by the TRMM satellite in three storm categories (DCC, WCC, and BSR, as defined in Section 2) to provide a seasonal spatial distribution of various types of severe weather impacts including floods, hail, and tornadoes (Figure 4). Other sources of disaster information for the region were explored (e.g., DesInventar database, www.desinventar.net), but were not used since such data are scarce and not commonly available for the TRMM era.

Flood reports are distributed throughout the region including Argentina and Uruguay, in both large population centers (e.g. Buenos Aires and Córdoba; labeled in Fig. 1i) and the relatively unpopulated La Pampa province in central Argentina (Figure 4a; labeled in Fig. 1a). Consistent with Figures 1, 2, and the seasonal distribution of TRMM storm probabilities [*Romatschke and Houze*, 2010], heavy rain and flooding tends to occur in central to eastern Argentina and Uruguay in the spring. These floods in the agriculturally rich Pampas region are typically slow-rise floods [*Latrubesse and Brea,* 2009]. Figure 2d indicates that they are likely produced by storms containing WCCs. Figure 5 of *Romatschke and Houze* [2010] shows that storms containing BSRs are most likely in this region. K. L. Rasmussen (manuscript in preparation, 2014) presents a spring-only version

of *Romatschke and Houze* [2010]'s storm type distribution that shows a similar location of BSRs in the Pampas region. Thus, the slow-rise floods in the east are likely associated with storms of extensive mesoscale organization both in their convective structure and their stratiform components. Figure 4a shows that during the summer, the flooding shifts northwestward toward the foothills of the Andes in Argentina and Bolivia. News reports indicate that these events are often flash floods. Figure 2b and e suggests that they could be associated with storms containing DCCs, WCCs, or both.

Figure 4b shows that reports of hail come from a west-east swath across Argentina from the Andes to the Atlantic coast. However, hail reports are highly concentrated in the extreme foothills of the Andes and Sierras de Córdoba, near the cities of Mendoza and Córdoba. Mendoza, located in the foothills of the Andes (32.9°S, 68.9°W; labeled in Fig. 1i), is greatly affected by frequent hailstorms with large hail (reported in newspapers as pea to grapefruit sized) that seriously impact the agriculture of this major wine-producing region (Fig. 4b). Many wineries in Mendoza have installed anti-hail nets and the Argentinian government subsidizes agricultural hail insurance and funds aircraft cloud-seeding efforts because of frequent large hail in the region [personal communication, Bodega Norton Winery, 2011]. Given the known distributions of lightning in the region close to the Andes foothills from Figures 1-3, frequent hail in the vicinity of the Andes foothills and the Sierras de Córdoba corresponds well to Figure 4b and is consistent with the findings of *Cecil and Blankenship* [2012]. Such a concentration of hail near mountains is unlike that in the United States [*Cecil and Blankenship,* 2012].

Echoing the findings of *Altinger de Schwarzkopf and Russo* [1982], but specifically looking at the most extreme storms seen by the TRMM PR in 16 years, Figure 4c

indicates the presence of a South American "tornado alley" in the central Pampas region. This region is far to the east of where hail is most frequent (Figure 4b); perhaps, mountainous terrain presents a boundary condition unfavorable to tornado dynamics [*Bosart et al.*, 2006; *Homar et al.*, 2003]. We also note that this region over the plains east of the Andes is where organized MCSs maximize in both frequency of occurrence and maturity [*Romatschke and Houze,* 2010; *Rasmussen and Houze,* 2011; *Salio et al.,* 2007]. More specifically, *Rasmussen and Houze* [2011] found that storms in this region that resembled the leading-line/trailing-stratiform archetype defined by *Houze et al.* [1990] were more likely to result in tornado reports, but they did not examine the mesoscale organization of storms containing DCCs in their study. Tornado reports shown in Figure 4c were associated with storms containing both DCCs and WCCs. Additionally, tornadic storms in the U.S. tend to be supercellular in structure with strong clockwise wind shear [*Maddox*, 1976; *Houze*, 2014] that is also present in subtropical South America [*Rasmussen and Houze*, 2011; counterclockwise shear in the Southern Hemisphere]. Thus, the specific characteristics of tornadic storms in subtropical South America need to be more closely examined in a future study to better compare to their more studied U.S. counterparts. However, consistent with known distributions of tornado activity in the U.S., tornadoes are most likely to form where more developed thunderstorms, supercells, and/or mature MCSs are located downstream of the mountain barrier.

5. Conclusions

The examination of various forms of severe weather in SSA in relation to TRMM Precipitation Radar data shows:

(1) The seasonal climatology of lightning in SSA has a maximum in spring and fall over northeastern Argentina and Paraguay in association with storms containing DCCs, WCCs, or both. In summer, the maximum of lightning frequency shifts southwestward to the foothills of the Andes, where it is associated with storms containing DCCs, WCCs, or both. The lightning in this region at this time of year tends to remain over the foothills and Sierras de Córdoba while mesoscale convective systems develop and spread eastward while continuing to build on their western sides as convection continues to generate over the lower mountains.

(2) A persistent nocturnal maximum of lightning activity is found over the foothills and Sierras de Córdoba in association with new convection, and with mesoscale systems that may continue to regenerate on their western sides while spreading eastward.

(3) Flooding occurs throughout SSA as a result of both flash floods near the foothills and Sierras de Córdoba, where storms with DCCs occur and slow-rise floods in the agriculturally-rich Pampas region, in association with storms containing WCCs. That is, the flash floods occur in the mountains with newly formed very intense and deep convection, whereas the floods over the plains occur in conjunction with mesoscale systems bearing horizontally extensive regions of intense convection and stratiform precipitation.

(4) Hail occurs throughout the region, but is highly concentrated in the Andes foothills and Sierras de Córdoba, near Mendoza, in association with storms containing DCCs or WCCs.

(5) A South American “tornado alley” is present in La Pampa region far to the east of the region of maximum hail occurrence. The tornado maximum is located where more developed and organized thunderstorms, supercells, and MCSs are likely to occur downstream of the Andes Mountains.

The findings from this study provide the basis for future research on severe weather and their impact in SSA. By integrating satellite radar and lightning data with ground-based storm reports to investigate the nature of extreme convective systems in SSA, a greater understanding of these storms, their role in the climate of the region, and their socioeconomic impact on local populations can provide crucial information that could save life and property in this vulnerable region.

Acknowledgements

Beth Tully coordinated the graphics. The authors would like to thank Dr. Daniel Cecil for insightful comments that have improved this manuscript. The authors would also like to thank Dr. Edward Zipser and an anonymous reviewer for comments that have improved this manuscript. The data used in this study were acquired as part of the NASA's Earth System Division. The TRMM PR data are distributed by the Goddard Earth Sciences (GES-DISC) Distributed Active Archive Center (DAAC). The LIS and OTD data are distributed by the EOSDIS Global Hydrology Resource Center DAAC. This research was sponsored by NSF Grant AGS-1144105, NASA Grants NNX13AG71G and NNX10AH70G, and a NASA Earth and Space Science Graduate Fellowship (NNX11AL65H).

References

Altinger de Schwarzkopf, M. L., and L. C. Russo (1982), Severe storms and tornadoes in Argentina, Preprints, *12th Conf. on Severe Local Storms*, San Antonio, TX, Amer. Meteor. Soc., 59–62.

Awaka, J., T. Iguchi, H. Kumagai, and K. Okamoto (1997), Rain type classification algorithm for TRMM Precipitation Radar, *Proc. 1997 Int. Geoscience and Remote Sensing Symp. (IGARSS '97)—Remote Sensing: A Scientific Vision for Sustainable Development*, Vol. 4, Singapore, IEEE, 1633-1635.

Bosart, L. F., A. Seimon, K. D. LaPenta, and M. J. Dickinson (2006), Supercell tornadogenesis over complex terrain: The Great Barrington, Massachusetts, tornado on 29 May 1995, *Wea. Forecasting*, **21**, 897-922.

Carey, L. D., S. A. Rutledge, and W. A. Petersen (2003), The Relationship between Severe Storm Reports and Cloud-to-Ground Lightning Polarity in the Contiguous United States from 1989 to 1998, *Mon. Wea. Rev*., **131**, 1211–1228.

Cecil, D. J., and C. B. Blankenship (2012), Toward a Global Climatology of Severe Hailstorms as Estimated by Satellite Passive Microwave Imagers, *J. Climate*, **25**, 687–703.

Cecil, D. J., D. E. Buechler, and R. J. Blakeslee (2014), Gridded lightning climatology from TRMM-LIS and OTD: Dataset description, *Atmos. Res*., **135-136**, 401–411.

Homar, V., M. Gaya, R. Romero, C. Ramis, and S. Alonso (2003), Tornadoes over complex terrain: An analysis of the 28th August 1999 tornadic event in eastern Spain, *Atmos. Res.*, **67-68**, 301-317.

Houze, R. A., Jr. (2014), *Cloud Dynamics*, *2nd Ed.*, Academic Press/Elsevier, 432 pp.

Houze, R. A., Jr., B. F. Smull, and P. Dodge (1990), Mesoscale organization of springtime rainstorms in Oklahoma, *Mon. Wea. Rev*., **118**, 613–654.

Houze, R. A., Jr., D. C. Wilton, and B. F. Smull (2007), Monsoon convection in the Himalayan region as seen by the TRMM Precipitation Radar, *Quart. J. Roy. Meteor. Soc*., **133**, 1389-1411.

Iguchi, T., T. Kozu, R. Meneghini, J. Awaka, and K. Okamoton (2000), Rain-profiling algorithm for the TRMM precipitation radar, *J. Appl. Meteorol*., **39**, 2038–2052.

Kummerow, C., W. Barnes, T. Kozu, J. Shiue, and J. Simpson (1998), The Tropical Rainfall Measuring Mission (TRMM) sensor package, *J. Atmos. Oceanic Technol*., **15**, 809-817.

Lang T. J., and S. A. Rutledge (2002), Relationships between Convective Storm Kinematics, Precipitation, and Lightning, *Mon. Wea. Rev*., **130**, 2492–2506.

Latrubesse E. M., and D. Brea (2009), Chapter 16. Floods in Argentina, *Dev. Earth Surf. Processes*, **13**, 333–349.

Macgorman D. R., and D. W. Burgess (1994), Positive Cloud-to-Ground Lightning in Tornadic Storms and Hailstorms, *Mon. Wea. Rev*., **122**, 1671–1697.

Maddox, R. A. (1976), An evaluation of tornado proximity wind and stability data, *Mon. Wea. Rev.*, **104**, 133–142.

Nascimento, E. L., and C. A. Doswell III (2005), The need for improved documentation of severe thunderstorms and tornadoes in South America, Preprints, *Symp. on the Challenges of Severe Convective Storms*, Atlanta, GA, Amer. Meteor. Soc., P1.18.

Rasmussen, K. L., and R. A. Houze, Jr. (2011), Orogenic convection in subtropical South

America as seen by the TRMM satellite, *Mon. Wea. Rev.*, **139**, 2399–2420.

Rasmussen, K. L., S. L. Choi, M. D. Zuluaga, and R. A. Houze, Jr., 2013: TRMM precipitation bias in extreme storms in South America, *Geo. Res. Lett.*, **40**, 3457–3461, doi:10.1002/grl.50651.

Romatschke, U., and R. A. Houze, Jr. (2010), Extreme summer convection in South America, *J. Climate*, **23**, 3761-3791.

Salio, P., M. Nicolini, and E. J. Zipser (2007), Mesoscale convective systems over southeastern South America and their relationship with the South American low-level jet, *Mon. Wea. Rev*., **135**, 1290-1309.

Xu, W., E. J. Zipser, Y.-L. Chen, C. Liu, Y.-C. Liou, W.-C. Lee, and B. J.-D. Jou (2012), An orography-associated extreme rainfall event during TiMREX: Initiation, storm evolution, and maintenance, *Mon. Wea. Rev*., **140**, 2555–2574.

Zipser, E. J., D. J. Cecil, C. Liu, S. W. Nesbitt, and D. P. Yorty (2006), Where are the most intense thunderstorms on earth, *Bull. Amer. Meteor. Soc*., **87**, 1057–1071.

Figure Captions

Figure 1. Monthly lightning climatology from the Lightning Imaging Sensor (LIS) and Optical Transient Detector (OTD) expressed as lightning rates (fl km^{-2} yr^{-1}) from September through May in SSA. The thick black line indicates the 0.5 km topography contour on the eastern Andean foothills.

Figure 2. Averaged lightning flash rates (fl min^{-1}) within TRMM-identified (a-c) deep convective cores and (d-f) wide convective cores showing the seasonal progression of lightning associated with extreme storms in South America. The thick black line indicates the 0.5 km topography contour.

Figure 3. Time-longitude diagrams representing the diurnal progression of averaged lightning rates (fl min^{-1}) within TRMM-identified (a) deep convective cores, (b) deep and wide convective cores, and (c) wide convective cores during the austral summer season (DJF). The diagrams are averaged over a meridional band bounded by 36°S – 28° S. Time in UTC and Mean Solar Time (MST) are displayed on the left and right ordinates, respectively. The black contour represents the average topographic relief in the latitude band defined above.

Figure 4. Severe storm reports derived from local media sources (newspapers in Argentina and Uruguay) showing the locations of (a) floods, (b) hail, and (c) tornadoes in SSA. Each symbol on all panels represents one report of each type of severe storm impact

separated into seasons (red – SON; blue – DJF; green – MAM). The topography is shaded in gray scale.

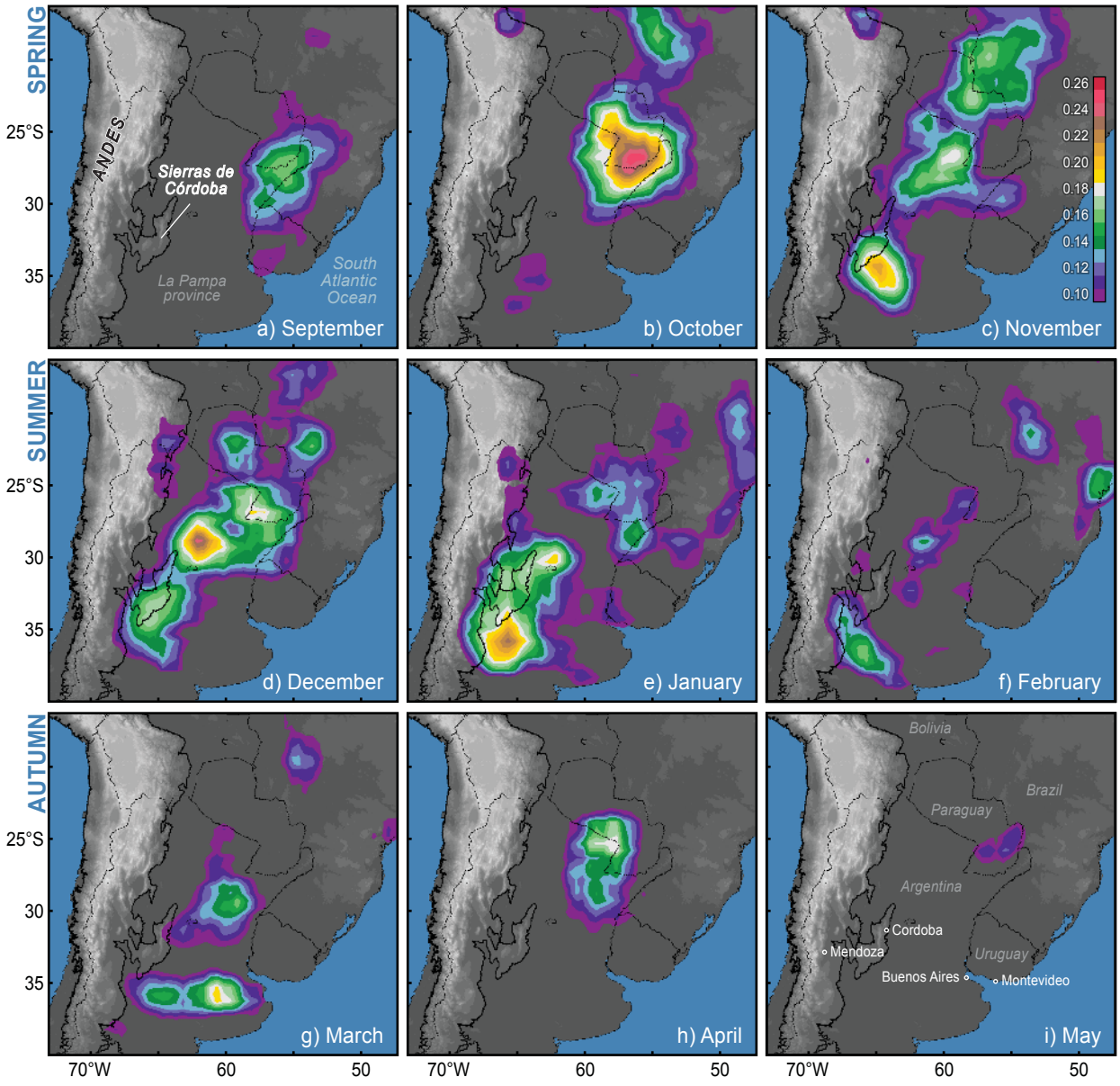

Figure 1. Monthly lightning climatology from the Lightning Imaging Sensor (LIS) expressed as lightning rates (fl km^{-2} yr^{-1}) from September through May in subtropical South America. The black line indicates the 0.5 km topography contour on the eastern Andean foothills.

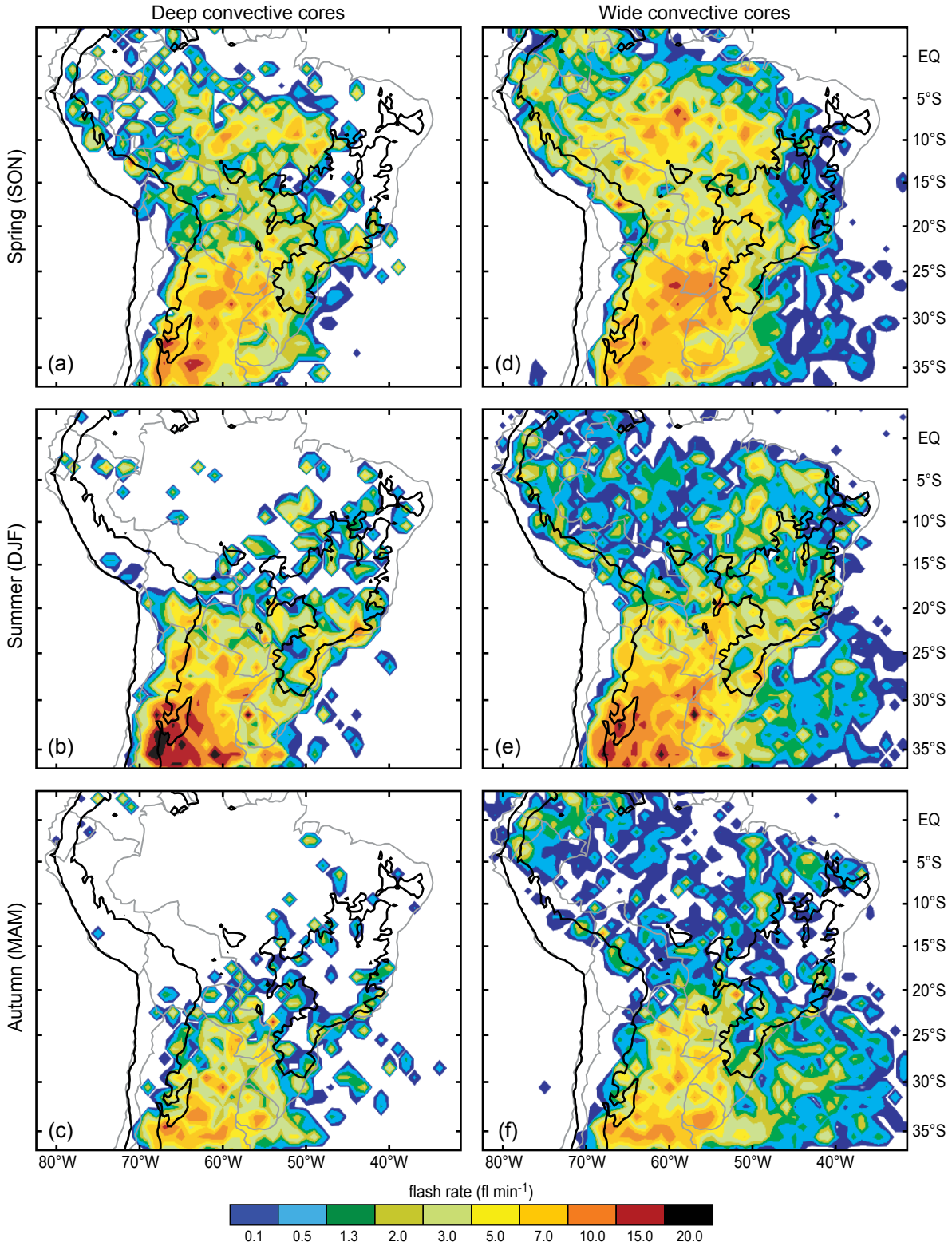

Figure 2. Averaged lighting flash rates (fl min^{-1}) within TRMM-identified (a-c) deep convective cores and (d-f) wide convective cores showing the seasonal progression of lightning associated with extreme storms in South America. The thick black line indicates the 0.5 km topography contour.

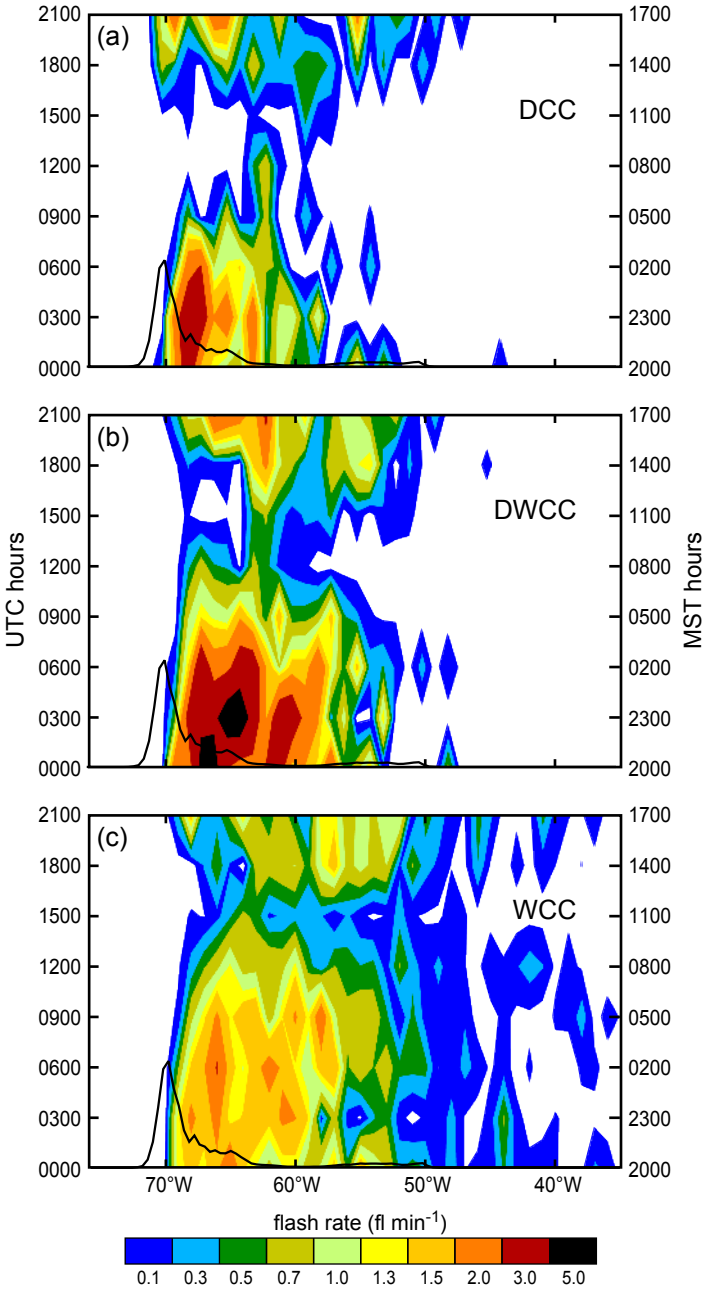

Figure 3. Time-longitude diagrams representing the diurnal progression of averaged lightning rates (fl min^{-1}) within TRMM-identified (a) deep convective cores, (b) deep and wide convective cores, and (c) wide convective cores during the austral summer season (DJF). The diagrams are averaged over a meridional band bounded by 36°S – 28° S. Time in UTC and Mean Solar Time (MST) are displayed on the left and right ordinates, respectively. The black contour represents the average topographic relief in the latitude band defined above.

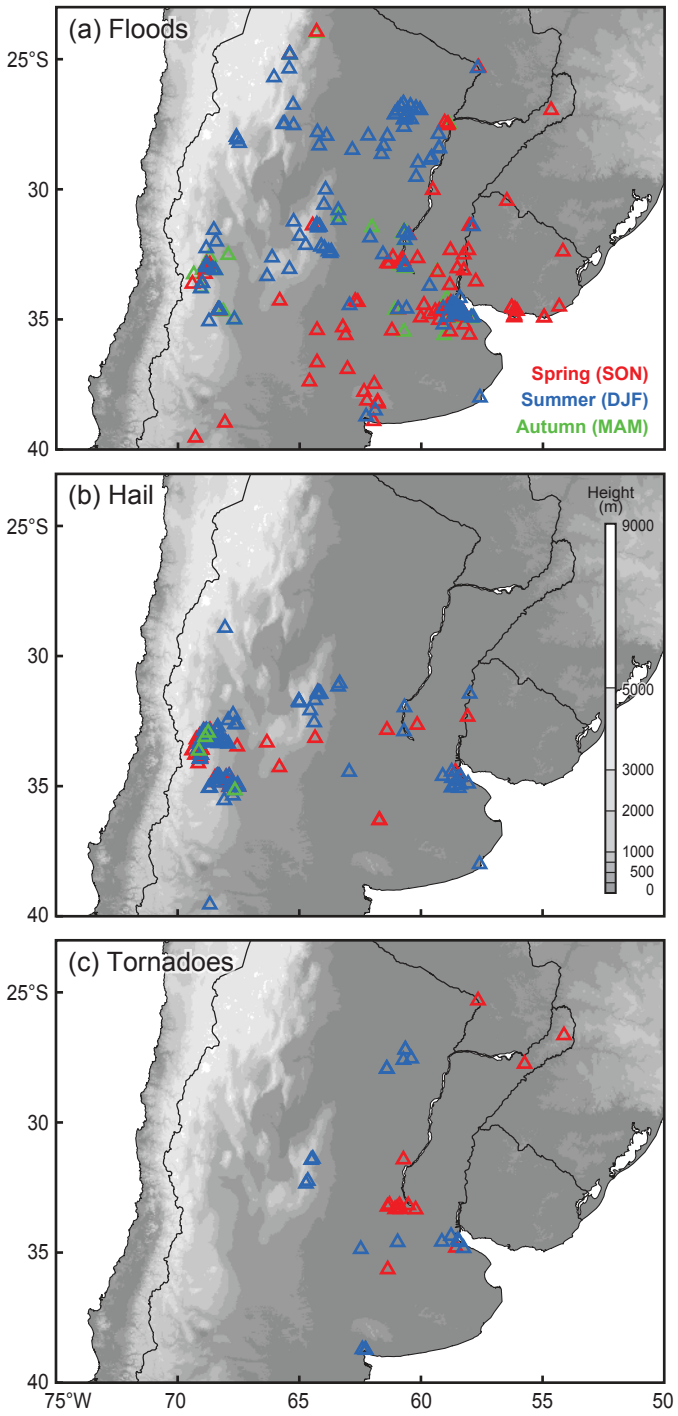

Figure 4. Severe storm reports derived from local media sources (newspapers in Argentina and Uruguay) showing the locations of (a) floods, (b) hail, and (c) tornadoes in subtropical South America. Each symbol on all panels represents one report of each type of severe storm impact separated into seasons (red – SON; blue – DJF; green – MAM). The topography is shaded in gray scale.